Clin. Vision Sci. Vol. 1, No. 3, pp. 245–256, 1987
Printed in Great Britain.

0887-6169/87 $3.00 + 0.00

THE ANALYSIS OF STEADY STATE EVOKED POTENTIALS REVISITED

HANS STRASBURGER
Institut fuer Medizinische Psychologie, Universitaet Muenchen, F.R.G.

(*Received* 13 *August* 1986; *in revised form* 12 *November* 1986)

Summary—1. This note provides a critical discussion of methods for the analysis of steady state visual evoked potentials.

2. To take advantage of the linearity of the Fourier transform, the results of submitting VEP data to a Fourier analysis are discussed in terms of a vector representation of the VEP frequency components.

3. Methods for averaging VEP data and for assessing VEP variability are described. "Vector averaging" of spectral data is found preferable over "scalar averaging."

4. The influence of noise on VEP amplitude is discussed.

5. Changes in temporal phase of the VEP response can be interpreted as changes in delay or latency provided the appropriate precautions in data analysis are taken.

6. Phase information can also be used to improve the VEP signal-to-noise ratio. This is the goal of phase-sensitive analysis.

7. Synchronous demodulation is a method for narrow bandpass filtering. It is shortly described.

8. Finally it is shown that the techniques of VEP analysis at issue are closely related; the correspondences are pointed out.

Key words—Evoked potentials; steady state; Fourier analysis; averaging; VEP reliability; signal-to-noise ratio.

INTRODUCTION

Since Campbell and Maffei's (1970) "electrophysiological evidence for the existence of orientation and size detectors in the human visual system", the technique of acquiring steady state visual evoked potentials (SSVEP) has gained increasing acceptance. The fact that steady state VEPs can be obtained at much higher recording speeds than transient VEPs made this technique a good candidate for application in basic research as well as in clinical context. Applications where the steady state method seems especially promising are those where the response to a *variation* of visual stimuli is of interest unlike the usual approach with transient stimulation where one tries to work with just a few, "ideal", stimuli.

Regan (e.g. 1975b, 1977b, c) has pointed out many such applications and has discussed methods for analysing the results (1977a, c). Except for his seminal work, however, the review and further development of methods for the analysis of SSVEPs has been largely neglected. Besides averaging, several other techniques of analysis have been used, the most important of them being Fourier analysis, narrow bandpass filtering, filtering based on synchronous demodulation, and phase-locked analysis. For the practical application this raises many questions. Which method is appropriate in a given case or should several be combined to ensure most efficient data processing? How can results from different methods be compared, and which of them gives the higher signal-to-noise ratio? What measures of reliability are available? What kinds of data representation are appropriate?

Thus the present study focuses on aspects that have been neglected in previous treatments of steady-state VEP analysis and which are not commonly found in signal processing textbooks. The material is presented in the form of a tutorial to aid readers unfamiliar with the field to make practical use of it.

First, since Fourier analysis and averaging are often used together (e.g. Campbell and Maffei, 1970; Florentini *et al.*, 1983; Petrig, 1980; and many others), their relationship is discussed. We will then discuss methods for averaging Fourier analysis results and address the hitherto neglected question of reliability of spectral data. These issues are easily treated when a vector representation of the Fourier analysis results is used. Such a representation, which is known from the theory of complex numbers, is also helpful in drawing conclusions for the influence of noise on SSVEP amplitude data. A discussion of the role of temporal phase leads to the concept of phase-locked analysis. The difference between phase-locked and phase-insensitive analysis is illustrated for the example of determining the contrast threshold by means of Campbell and Maffei's (1970) regression technique, and data is shown. Finally it is shown how the various methods for SSVEP analysis [averaging, Fourier analysis of averaged and non-averaged data, narrow band-pass filtering, and phase-locked (synchroneous) filtering], can be classified into phase-locked and phase-insensitive methods. A more rigorous use of signal processing concepts allows for avoiding confusion (e.g. Regan 1977a, c) between such techniques.

The idea of analysing few VEP parameters in response to a wide variety of stimuli rather than trying to extract a lot of information from responses to just a few stimuli can be taken one step further by applying a sweep technique. Well known in electrical engineering, sweep techniques have been introduced to the acquisition of VEPs by Regan (1975a) and Tyler (1979). The data analysis techniques discussed in the present report can all be used together with swept stimulation. A discussion of sweep techniques is omitted in the present report, however, since it seems more concerned with stimulus presentation techniques than with data analysis. The reader is referred to Strasburger and Rentschler (1986) where we describe a practical VEP acquisition system taking into account the issues of the current report.

SPECTRAL ANALYSIS OF STEADY STATE VEP

At the outset it seems appropriate to define the precise difference between transient and steady state stimulation. The distinction is not clear cut, however. In transient stimulation, one attempts to capture the EEG response to a single event yet one uses repeated stimulation as a means to enhance the generally small response. In the other case, the visual system is repeatedly stimulated with a higher temporal rate in an attempt to put it into a "steady state"; rhythmical EEG components are then taken as response. To differentiate the two methods one might define a critical stimulation period taken as the time after which a response has decayed (*ca* 500 ms). There are, however, methods available for obtaining a transient response at higher stimulation rates. It is more the intended *response* description—in the time domain, or in the frequency domain—which distincts transient from steady-state stimulation; both methods should be viewed as complementary for investigating a given dynamic system.

Since a periodic stimulation is most sparsely described in the frequency domain it seems natural to also describe steady state results in the frequency domain. As a common way of analysis, however, the averaging procedure familiar from transient VEPs is used for analysis with the period T set to an integer multiple of the stimulation period (e.g. Campbell and Maffei, 1970; Fiorentini *et al.*, 1983; Petrig, 1980). Figure 1(a) shows an example of an averaged SSVEP which had been obtained with a low sampling rate. Like in the example, the resulting VEP often resembles a sinusoidal wave-form with twice the frequency of the stimulation frequency. This type of response does not necessarily reflect the spectral purity of the underlying signal, but is brought about by the fact that averaging acts as a *comb filter*, comparable to a combination of several narrow band pass filters tuned to integer multiples of the averaging frequency $1/T$. With a stimulation rate of 8 Hz and an averaging period of 125 ms as in Fig. 1(a), only frequency components of 8, 16, 24 Hz, etc. pass through the averaging filter. In case that the signal is sent through a low-pass filter with a cutoff frequency of, say, 22 Hz, then there remain only a 16 Hz component and an attenuated 24 Hz component. Yin *et al.* (1983), for example, use a bandpass with corner frequencies of 12 and 22 Hz. The sinusoidal purity of their signal stems from averaging and is not mainly brought about by the steepness of their analog filters, as they assume.

For estimating the strength of the averaged signal, peak and trough amplitudes have been measured similarly to the common analysis of transient VEPs (see for example Campbell and Maffei, 1970). Yet, since the higher harmonics that pass through the comb filter contaminate the result, Fourier analysis of the averaged signal has been advocated (Regan, 1977a). This is illustrated in Fig. 1(b), (c) which shows amplitude and temporal phase data for the averaged signal of Fig. 1(a).

Here the question arises whether these two methods, Fourier analysis and averaging, some-

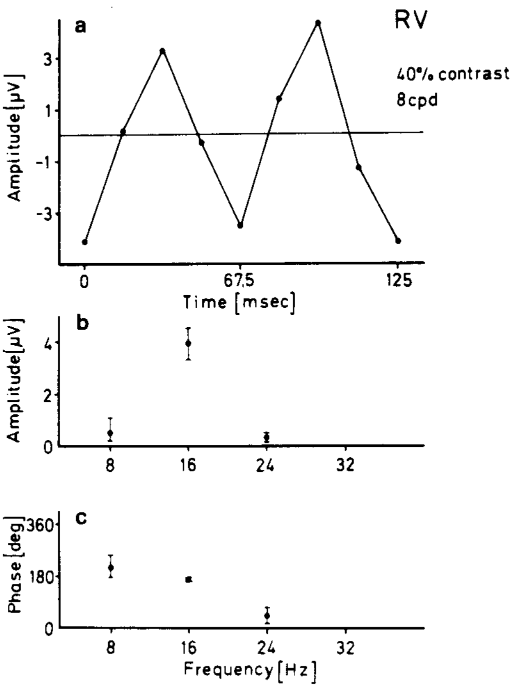

Fig. 1. A plot of an averaged SSVEP (a) and its spectral content (b) and (c). Stimulus modulation frequency is 8 Hz (16 rps) and a low sampling rate of 64 Hz has been chosen since it suffices to capture the spectral energy up to the 3rd harmonic (24 Hz). Note that the "jagginess" in the temporal plot resulting from the low sampling rate has no effect on the accuracy of spectral data. The lowest occurring frequency (8 Hz) is related to the chosen temporal window (125 ms). No information is present at the Nyquist frequency (32 Hz).

how interact and whether, perhaps, the Fourier analysis should be enacted on the raw signal directly. The issue is resolved by the assertion that both averaging and Fourier analysis are linear operations, so that the order in which they are applied is irrelevant. In other words, a Fourier transform of an averaged signal yields the same result as the average over Fourier transforms which are enacted on the individual sections S_i of length T. Note that a Fourier transform of a signal of length T, like averaging, yields only spectral components which are integer multiples of $1/T$, resulting in the same number of components. In our example this section of length T is quite short (125 ms), and so there are only a few resulting components.

The quantity $1/T$ is termed "frequency resolution." It is also the lowest frequency component that can occur. When, for example, a stimulation rate of 8 Hz and an averaging section length of 125 ms are used, the lowest occurring frequency will be the stimulus fundamental of 8 Hz, showing as one period of a sine wave in the averaging window of Fig. 1. Sometimes investigators have used a longer averaging section length to cover several stimulation cycles. The resulting averaged wave forms then show several response cycles of the fundamental, where a difference in the relative height of these cycles reflects the presence of a lower frequency component (i.e. a subharmonic).

AVERAGING OF SPECTRAL DATA

Polar representation of FFT results

For the following description of methods for averaging spectral data, a polar representation of spectral data is most convenient. Fourier analysis is usually based on calculating a digital Fourier transform of the sampled signal using an algorithm called the Fast Fourier Transform (FFT). The result is a set of pairs of amplitude and phase angle values with each amplitude/phase pair corresponding to a particular frequency component. The total number of components is $(n/2)$-1 plus a D.C.-component, with n denoting the number of sample points. Thus, each component constitutes a vector $\mathbf{s} = (x, y)$ in a two-dimensional domain with the length of amplitude A and the orientation of (temporal) phase angle ψ. Alternatively, the data can be described by using the projections of these vectors onto the axes of the plane of complex numbers

$$x = A \cos(\psi)$$

$$y = A \sin(\psi).$$

For reconversion, the phase angle is obtained by using the arctangent of y/x, and the amplitude is given by the Pythagorean theorem.

A polar representation is also useful for representing experimental results, since it combines amplitude and phase information in one graph. Figure 2(b) shows results from an experiment where subjects were presented with phase-alternating sine-wave gratings of varying spatial frequency (i.e. varying bar width). The graph shows the 2nd harmonic component (16 Hz). It can be seen that the temporal phase increases monotonically with increasing spatial frequency, and amplitude first increases to reach a maximum, and then decreases.

Vector averaging of frequency components and reliability

The linearity of the Fourier transform is obvious from its definition. The linearity applies,

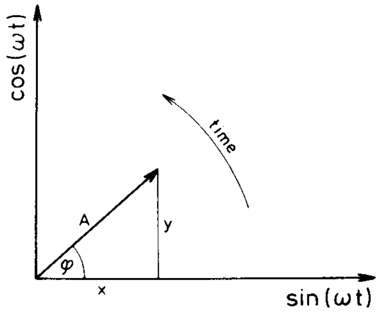

(a)

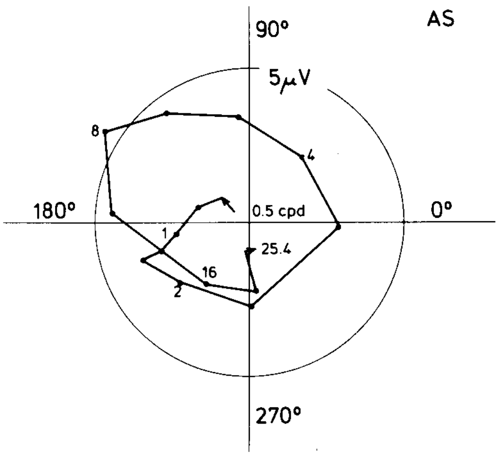

(b)

Fig. 2. Polar representation of spectral data. Subject A.S. is a 27-year-old emmetropic female with Landolt-C acuity of 1.3, binocularly viewing vertical sine-wave gratings of varying spatial frequency. Pattern contrast is sinusoidally modulated at 8 Hz resulting in stimuli where light and dark bars interchange at 16 reversals per second. The 16-Hz component from a spectral analysis is plotted in dependency on pattern spatial frequency.

however, only to the sine/cosine representation (both the arctangent and the r.m.s.-function are highly non-linear, i.e. not even well aproximated by a linear function). Consequently, for averaging over the same frequency component from several signal sections S_i, *vector addition* has to be used. If (x_i, y_i) is a given frequency component of section S_i, the average component is obtained by

$$(X, Y) = ((\Sigma x_i/n), (\Sigma y_i/n)) \quad i = 1, n.$$

The resulting phase angle is

$$\Phi = \arctan\,(Y/X).$$

To assess how meaningful differences in spectral results obtained under different experimental conditions are, it is necessary to have a measure of statistical variability. Surprisingly, reliability results have been omitted in most experimental SSVEP studies. Using a polar representation, it is, however, straightforward to derive a useful measure.

Let s_x and s_y denote the standard deviations of x_i and y_i, respectively

$$s_x^2 = \frac{\Sigma(x_i - X)^2}{n-1} \quad s_y^2 = \frac{\Sigma(y_i - Y)^2}{n-1}.$$

The variability of the mean projections X and Y decreases with increasing n with the square root of n, and so the standard errors are given by

$$s_X = s_x/\sqrt{n} \quad s_Y = s_y/\sqrt{n}.$$

A deviation vector $\mathbf{D} = (s_x, s_y)$ can be defined which has the length

$$\text{length }(\mathbf{D}) = \sqrt{s_x^2 + s_y^2}$$

and the angle

$$\text{angle }(\mathbf{D}) = \arctan\,(s_y/s_x).$$

It can be seen from Fig. 3, however, that this vector $\mathbf{D}$ cannot directly be used as a measure of amplitude and phase variability, since it does not necessarily point in the same direction as (X, Y).

According to the Central Limit Theorem (e.g. Hays, 1963) the means X and Y will be asymptotically normally distributed for sufficiently large n, so that it is possible to calculate an interval of confidence for the means X and Y by

$$c_X = \pm 1.96 \cdot s_x/\sqrt{n}$$

and

$$c_Y = \pm 1.96 \cdot s_y/\sqrt{n} \quad (P = 5\%)$$

In other words, with a probability of 95% the mean vectors will point inside a rectangle of size $2c_X \cdot 2c_Y$ with the center (X, Y) (Fig. 3).

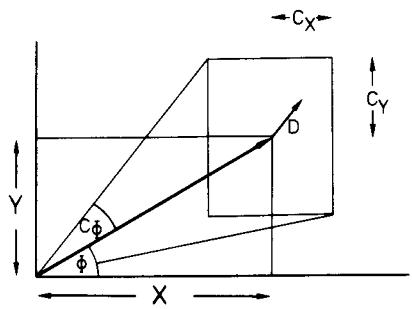

Fig. 3. Confidence intervals for the mean projections X and Y, and for the mean amplitude and mean phase.

Thus, a conservative estimate of the interval of confidence for the amplitude is half the rectangle's diagonal

$$c_A = \pm 1.96 \cdot \sqrt{s_X^2 + s_Y^2}.$$

For a less conservative estimate one can calculate the vector sum of (X, Y) and $1.96 \cdot \mathbf{D}$

$$\sqrt{(X - c_X)^2 + (Y - c_Y)^2} \leqslant A \leqslant$$

$$\sqrt{(X + c_X)^2 + (Y + c_Y)^2}.$$

If the rectangle does not overlap with the coordinate system's origin then the mean vector is significantly different from zero. In this case an interval of confidence c_ϕ for the mean component's phase angle can be derived, which is most easily done geometrically from Fig. 3.* A still less conservative method could use a two-dimensional normal distribution for the x_i, y_i, leading to a confidence ellipsis rather than a rectangle.

In calculating the signal to noise ratio of FFT results, the value corresponding to the number of repetitions in conventional averaging is the number n of stimulation periods. It is directly related to the total duration t of the recorded signal

$$n = t/T$$

where T is the stimulation period. This is true independently of whether averaging, the FFT, or a combination of both is used. When Fourier analysis is used, the improvement of the signal to noise ratio is also reflected in frequency resolution, which is (roughly) the bandwidth of frequencies of the original signal contributing to a certain frequency component. This frequency resolution is expressed as

$$\Delta f = 1/T$$

T denoting the duration over which the FFT was calculated.

When the analysis is set up such that Fourier analysis is performed *after* averaging, it is still possible to obtain reliability data by running several trials. The FFT is then performed over each averaged trial separately and the resulting components are submitted to vector addition. As a consequence of linearity, the same rules apply as stated before. n, in this case, is the number of trials used.

Scalar averaging of spectral components

A method different from vector averaging described above is used more commonly for averaging spectral data. In what I call "scalar averaging", amplitude values are used directly for averaging instead of using the projections; i.e. if, for a given frequency, A_i denotes the component's amplitude for a Fourier transform of the signal section S_i, one defines

$$A = \Sigma A_i/n \quad i = 1, n.$$

A mean phase is usually not calculated, but one could similarly try to define

$$\Phi = \Sigma \psi_i/n \quad i = 1, n.$$

Although this method seems simpler at first sight, two difficulties arise here. First, since taking the length of a vector is a non-linear operation, the useful property of averaging and Fourier transformation commuting does not apply and the mathematical properties of the results are less obvious. Second, the mean phase is not uniquely defined by the above formula due to the circular nature of angles. Suppose as an illustration that there are two phase angles $\phi_1 = 10$ deg and $\phi_2 = 350$ deg. Obviously, a mean of 0 deg is meaningful, but simple averaging would yield 180 deg. To use the mean angle as a measure of the central tendency of a set of angles, one can determine the smallest range within which all angles lie ([−10, +10] in the example), and express all angles within this range prior to averaging (adding or subtracting 360 deg where necessary). Note that this is *not* identical to taking all angles modulo 360 deg. The difficulties with scalar averaging are most prominent for noisy signals or when the number of trials is large. This is illustrated in Fig. 4. When all phase angles lie in a small range, scalar and vector averaging give similar results. For a range of angles of 90 deg, and constant amplitude, the two phase means differ by less than 1 deg (Batschelet, 1965, p. 15).

---

*Batschelet (1965, p. 13) and Zar (1974, p. 314) give another reliability measure for angles, the measure of dispersion of angles s for circular distributions

$$s = \sqrt{2(1 - r)} \text{ with}$$

$$r = (1/n)\sqrt{(\Sigma \cos \psi_i)^2 + (\Sigma \sin \psi_i)^2}.$$

This is, however, not applicable in our case. Since amplitudes are specified, phase angles should not be treated as circular distributions. A more detailed discussion of the statistical properties of circular distributions can be found in Batschelet (1965) and Zar (1974). Note that we now have *three* notions of a mean angle: the two definitions given for vector and scalar averaging, and the concept of a mean angle for a circular distribution, where individual angles are not weighted by amplitudes

$$\Phi = \arctan\,[(\Sigma \sin \psi_i)/(\Sigma \cos \psi_i)].$$

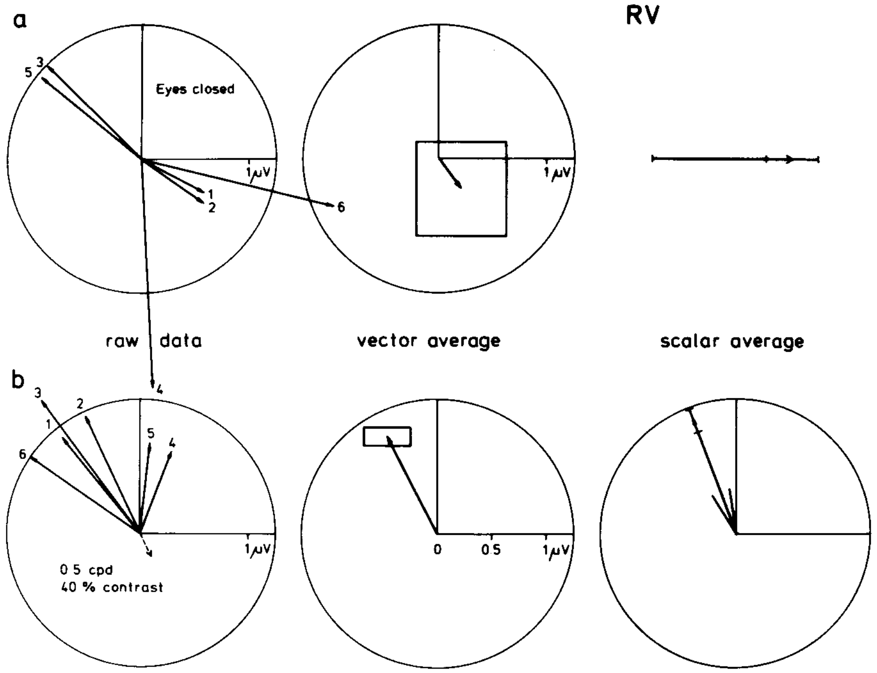

Fig. 4. The different effects of vector and scalar averaging are illustrated for recordings with (a) high and (b) low noise present. The figure shows 16 Hz component data from six 2-sec trials recorded from a 28-yr-old emmetropic female subject. In the high-noise situation (a), the subject has her eyes closed; the low-noise recording in (b) is obtained by stimulating with 8 Hz phase-alterating sine-wave gratings having 40% contrast and 0.5 c/deg spatial frequency. A vector average can be obtained in both cases (middle row) whereas a mean phase angle is not uniquely defined for scalar averaging of noisy data (upper right). Note, however, that even with low noise, the calculation of a scalar mean angle may be difficult, since a single small vector pointing away from the vector bundle [as indicated by the dashed arrow in (b)] may render the determination of a smallest range impossible, unless some additional assumption is introduced. In the case of vector averaging, the presence of high noise in (a) shows itself by the resulting vector having a small amplitude so that the confidence interval overlaps with the origin.

Influence of noise on amplitude data

It is interesting to apply the vector representation to the question how noise will influence amplitude data. Due to the non-linearity of the r.m.s. operation it will turn out that noise has a more pronounced influence on small signals than on strong ones.

The SSVEP can be thought of as the vector sum of an underlying signal **s** and a noise vector **r**. Let us assume that the noise vector is statistically independent of the signal (the phenomenon of the alpha-blockade, i.e. the suppression of EEG alpha activity for eyes open, shows that this is not always a valid assumption), and is uniformly distributed (i.e. its vector average is zero). The SSVEP **v** was derived as the vector sum of the FFT results for the signal segments. Let the individual vectors $\mathbf{v}_i = (x_i, y_i)$ be composed from signals $\mathbf{s}_i$ and noise vectors $\mathbf{r}_i = (x_{ri}, y_{ri})$. The law of commutativity implies that the signal **s** is the vector sum of the individual vectors $\mathbf{s}_i$, and the noise vector **r** is the vector sum of the r_i.

$$\text{SSVEP} = \mathbf{v} = \mathbf{s} + \mathbf{r}$$

$$\mathbf{s} = \Sigma\, \mathbf{s}_i/n$$

$$\mathbf{r} = \Sigma\, \mathbf{r}_i/n.$$

Since according to the Central Limit Theorem the means of the noise-projections x_{ri} and y_{ri} decrease with the square root of the number of trials n, the *amplitude* of the mean noise vector will also decrease with $\sqrt{n}$.

We can now look at how noise influences small or strong signals. We illustrate this at the dependency of SSVEP amplitude on pattern contrast, where we obtain both high and low signal amplitudes (Fig. 5). This example is of particular interest because the VEP threshold obtained by intersecting the regression line in

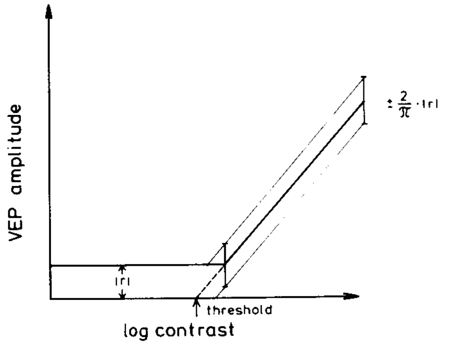

Fig. 5. VEP amplitude vs log contrast. r denotes the average noise vector. Note that the variability at low contrast levels is greater by a factor of $\pi/2$. The dotted line denotes linear regression.

this plot with the horizontal axis is a good predictor of the perceptual threshold (Keidel, 1965a, b; Campbell and Maffei, 1970). For high contrast values, SSVEP amplitudes of several microvolts are obtained. With decreasing contrast, VEP amplitude decreases more or less monotonically. At a certain contrast level still above the threshold, the signal will be smaller than the noise, and the amplitude plot will level out to a line parallel to the x-axis.

In the low contrast range of Fig. 5, the response function represents noise amplitude and will thus decrease with the square root of the number of trials. Now, what does the amplitude reponse function look like for medium contrast, near the intersection of the regression line with the x-axis, where a small signal buried in noise is present, or for high contrast where the signal is (presumably) large compared to the noise?

Consider first a signal $\mathbf{s}$ which is large compared to noise (i.e. the right part in Fig. 5). Let $\mathbf{r}_s$ be the projection of the noise vector onto the signal, and $\mathbf{r}_p$ the component perpendicular to this. The amplitude A can be decomposed as

$$A = \sqrt{(|\mathbf{s}| + \mathbf{r}_s)^2 + \mathbf{r}_p^2}$$

where $|\mathbf{s}|$ denotes the amplitude of $\mathbf{s}$. Since noise was assumed as small, $\mathbf{r}_p^2$ can be neglected, and the equation becomes

$$A = |\mathbf{s}| + \mathbf{r}_s.$$

Therefore only the projection of the noise vector onto the signal vector contributes to the measured amplitude. The variability of the amplitude is not given by the noise amplitude (as might be expected) but by its average projection onto the signal, which is $(2/\pi)\cdot|\mathbf{r}|$ for circularly uniformly distributed noise (i.e. noise where all angles have equal probability).

Consider next a signal $\mathbf{s}$ which is small compared to the noise (i.e. the center part in Fig. 5). Now let $\mathbf{s}_r$ be the projection of the signal onto the noise vector $\mathbf{r}$ at this point, and $\mathbf{s}_p$ the signal's perpendicular projection. The amplitude A can then be decomposed as

$$A = \sqrt{(\mathbf{s}_r + |\mathbf{r}|)^2 + \mathbf{s}_p^2}.$$

Since $|\mathbf{s}|$ is already small compared to $|\mathbf{r}|$, $\mathbf{s}_p^2$ can be neglected and the equation becomes

$$A = \mathbf{s}_r + |\mathbf{r}|.$$

Only the projection of the signal onto the noise vector contributes to the measured amplitude. Depending on the angle between signal and noise, the amplitude will be above or below noise level.

Summarizing the influence of noise on amplitude, we find that, due to the nonlinearity of the r.m.s.-function, noise has less influence on the amplitude of strong signals than might be expected, only its projection onto the signal contributing to variability. Similarly, for small signals, the *signal* will be underestimated, since only its projection onto noise contributes to the measured amplitude.

INTERPRETATION OF TEMPORAL PHASE

Whereas for transient VEPs the latency data are considered more useful than amplitude data, the temporal phase of steady state VEPs, which is the corresponding parameter, has received little attention. Moreover, the ambiguous nature of its absolute values has often been overlooked. Levi and Harwerth (1978, Fig. 3), for example, wanted to demonstrate an increase in temporal phase, corresponding to an increase in latency, for increasing spatial frequency, but they plot phase such that between adjacent points there is an increment of more than 360 deg. On one hand temporal phase results have such been over-interpreted, but on the other hand their interpretation was short stepped when any relationship between phase and latencies gathered from transient VEP recordings was denied. The argument is usually founded by reference to the fact that the system underlying steady state evoked potentials is highly nonlinear. Although linearity of the system is a sufficient condition for phase/latency conversion, it is not a necessary one.* Non-linearities result in changing the spectral content of the output signal (adding for example components that were not present in the input signal) but do not influence the phase of a given component. A full-wave rectifier with an ideal parabola transfer function, for example, adds a second harmonic and, given a certain input amplitude, completely suppresses the fundamental. Yet the phase of the second harmonic is in a static temporal relationship with that of the fundamental. A sounder argument is based on a model where the visual system is conceptualized as being composed of a pure delay system (corresponding to the optical nerval pathways) in series with an oscillatory system (corresponding to higher visual processing in the cortex) (e.g. Spekreijse *et al.*, 1977). In this model, the first observable response in the transient VEP would correspond to the pure delay system, while the temporal phase from the SSVEP would also include the delay from the oscillatory system. Nevertheless, it is still possible to convert the SSVEP phase angle into this overall delay time, as long as one keeps the different meaning between the two delay time measures in mind. When it comes to relating VEP delay times to psychophysical reaction time data, it might be speculated that SSVEP delays could yield better predictions of the psychophysical behavior, since a greater part of the visual system is involved. It remains an empirical question in any case, what relation exists between transient latency times and SSVEP phase angles.

Although phase angles are only defined modulo 360 deg, it is still possible to show relative phase differences exceeding 360 deg. This is done by continuously changing an additional variable in a sweep technique, in which case we can assume that phase will also vary continuously. In a discrete sweep technique (i.e. where several stimuli are shown quickly one after the other), the step width in the swept variable must be chosen to be small enough. Figure 6 illustrates how to proceed. The spatial frequency of sinewave grating stimuli is the swept variable in this case. Arbitrarily choosing the first point (for 0.5 c/deg), each succeeding point to the right is transformed (by adding/subtracting 360 deg) such that its distance to the preceeding point is minimized. If such a choice is not possible, the measurement has to be repeated with a smaller step-width.

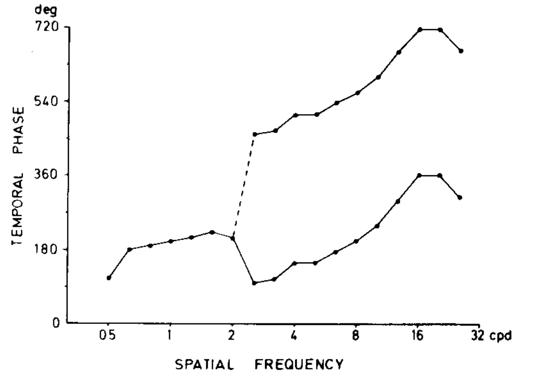

Fig. 6. Construction of a temporal phase plot. The phase value corresponding to the first data point is arbitrarily allocated to the interval of 0–360 deg. The phase value corresponding to each succeeding spatial frequency value is then determined by minimizing the distance to the preceeding point, adding or subtracting 360 deg when necessary. In this example there is a certain ambiguity at 2 c/deg since the standard deviation of this point is quite large relative to the other points. It is not clear whether a step of −108 deg to the lower curve, or a step of +252 deg to the upper trace should be chosen. An additional measurement between 2 and 2.5 c/deg could resolve this uncertainty.

PHASE-LOCKED ANALYSIS

Besides studying temporal phase in its own right, phase data can also be used to help in the analysis of amplitude by improving the signal to noise ratio. Assuming that the noise's phase angle is independent and generally different from the phase of the signal, one can improve the signal to noise ratio by restricting the analysis to the phase angle which is known to be the one of the signal in interest. This is the idea underlying phase-locked analysis techniques.

The restriction to a certain phase is done by using the projections onto some predefined phase which is assumed to be that of the signal. Let us illustrate this again at the example of the SSVEP's dependency on contrast.

For high contrasts, the VEP phase angle will be mainly determined by the underlying signal.

*For a linear system the concepts of latency and temporal phase of a given frequency component are equivalent modulo 2π

$$\psi = \tau \cdot f \cdot 2\pi \pm k \cdot 2\pi$$

where ψ is phase in radians, τ is latency in seconds and f is frequency. So for a given phase value to derive the corresponding latency a certain number of full periods 2π have to be added or subtracted. Diamond (1977) provides a different conversion method based on the slope of the phase vs temporal frequency function.

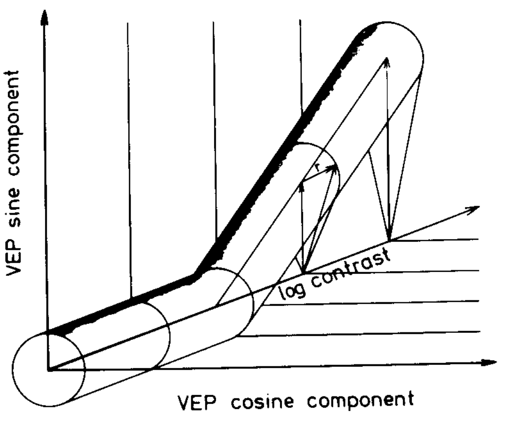

Fig. 7. Vector representation of VEP vs log contrast. The horizontal and vertical axes span the complex plane of FFT results. The contrast axis points away from the observer. The complex plane is rotated around the contrast axis such that the mean phase angle for suprathreshold values points upwards. Noise vectors lie within a cylindrical tube around the signal curve. Resulting vectors (signal + noise) do not exactly point upwards but lie within a V-shaped range. One sample vector is shown. Note that in contrast to Fig. 5, the vertical axis is not amplitude. VEP amplitude is given by the length of the vectors. Thus, an amplitude plot can be derived by rotating all resulting vectors upwards.

If it is assumed that the signal's phase angle is independent of contrast changes, the variability in phase angle in the right half of Fig. 5 is solely brought about by background noise. With this assumption it is warranted to calculate a mean phase angle Φ for suprathreshold contrasts and thus the data leading to Fig. 5 can be replotted in such a way that the projections of the VEP onto this mean phase angle are drawn. This is performed schematically in Fig. 7, where the phase angle is drawn in a third dimension perpendicular to the plane used in Fig. 5. For the sake of clarity, the coordinate system has been rotated such that the mean phase angle Φ points upwards.

Because the projections of the noise vectors onto the signal phase will always be smaller than the noise vector's amplitude, this will lead to an improvement of the signal to noise ratio.

Two observations can be made here. The phase-lock is not absolute as Regan (1977a, p. 114) for example assumes. Unwanted signals rather contribute with the cosine of their phase difference from the measurement phase. Second, phase-locked analysis only leads to a significant improvement of the signal-to-noise ratio for low signal amplitudes! This can be seen by comparison to our previous observations about signal/noise decomposition. For high amplitudes, phase-locked measurement does *not* lead to a S/N-improvement.

If the signal phase is *not* constant during a measurement, e.g. if the phase depends systematically on contrast in a contrast sweep experiment, the projections onto phase angles obtained at high-contrast lead to an underestimation of low contrast signals. This leads to the regression lines having a steeper slope and predictions of higher threshold contrasts (= lower sensitivity). In sum, phase-locked analysis will yield more reliable but possibly too low contrast threshold estimates.

Figure 8 shows a contrast sensitivity function for one subject together with VEP thresholds from amplitude and projected data. In a series of experiments conducted to study the dependency of SSVEPs on spatial frequency and contrast (Strasburger *et al.*, 1986) we found phase variations in the order of 60 deg for a change of contrast from 40 to 10%. This leads to an underestimation of VEP amplitude of 50% at 10% contrast for projected (= phase-sensitive) data. Threshold sensitivity is then underestimated by approximately 0.5 log units.

The relative merit of phase-sensitive analysis thus depends critically on the independence of phase from the swept variable. A more refined procedure would not assume a constant reference phase but had the reference phase be a function of the swept variable. If such a systematic relationship can be established, the underestimation of the signal from using a "wrong" phase can be avoided. This would combine the higher S/N ratio of phase-locked analysis with the better precision of phase-insensitive analysis.

SYNCHRONOUS DEMODULATION

Synchronous demodulation is a method for narrow bandpass filtering. It is shortly described here for its close relatedness to the other discussed techniques (for a thorough discussion of synchronous demodulation techniques see Nelson *et al.*, 1984). The method is widely used for steady-state VEP analysis (e.g. Tyler, 1978; Regan, 1975a) but is usually not specifically named. The term *synchronous demodulation* was introduced to evoked potentials work by Nelson *et al.* (1984) from electrical engineering applications literature. Another term for this kind of device is "heterodyne filter".

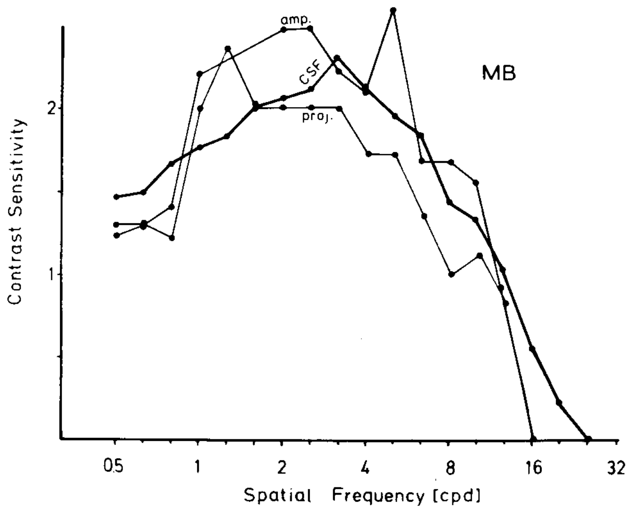

Fig. 8. Psychophysical contrast sensitivity function (CSF) for one subject together with VEP thresholds from amplitude data and phase-locked (projected) data. Projected data tends to underestimate the psychophysical CSF as a consequence of phase variations.

For a time dependent input signal $I(t)$, two signals $X(t)$ and $Y(t)$ are calculated in real time by multiplying the input with an externally supplied sine and cosine wave, and subsequently integrating with a low-pass filter

$$X(t) = \int_{t-T}^{t} I(\tau)\cos(\omega\tau)\,d\tau$$

$$Y(t) = \int_{t-T}^{t} I(\tau)\sin(\omega\tau)\,d\tau.$$

These calculations extract those components from the input signal having their frequency and phase close to those of the reference signal. The reference frequency and phase are chosen appropriately by the experimenter. The integration over a fixed length moving time window in the preceeding formula is only an approximation to the action of a low-pass filter. More precisely, the input function is weighted with a continuous function prior to integration which decreases for time points further in the past.

From these signals X and Y, a polar signal representation can be derived in a subsequent "*quadrature*" circuit

$$A(t) = \sqrt{X^2(t) + Y^2(t)}$$

$$\psi(t) = \arctan\,[Y(t)/X(t)].$$

From their definition it can be seen that these calculations represent an aproximation to one frequency component in a Fourier analysis, calculated over a moving time window in real time. Most of what has been said before therefore applies here as well. Unlike in a Fourier analysis, however, which is calculated step-wise over non-overlapping time sections of duration T, in synchronous demodulation the time windows overlap. A sudden change in the input signal will thus only slowly change the output. Whereas Fourier analysis yields results once every T seconds, synchronous demodulation gives continuous results but the effects are "smeared" over time.

The calculations are usually performed by analog circuitry. An electronic piece of equipment performing such calculations is often called a *lock-in amplifier*. In the simplest case, it provides a square-wave instead of a sine wave as a reference signal since then the multiplication is reduced to a simple switching of signal polarity. Such a unit acts as a parallel bank of synchronous filters with center frequencies and gains following the overtone series of a square-wave. More sophisticated units supply a range of reference signals and allow for automatic determination of the reference phase (using a phase-locked loop circuit).*

*Such units are, for example, manufactured by Princeton Applied Research, Princeton, N.J., or Ithaco, Ithaca, N.Y. The high technical specifications of these units are, however, not required for evoked potentials analysis.

CORRESPONDENCE BETWEEN ANALYSIS TECHNIQUES

Several different analysis techniques to determine SSVEP amplitude are in common use.

Campbell and Maffei (1970), for instance, use conventional analog bandpass filtering, Fiorentini *et al.* (1983) and Petrig (1980) use Fourier analysis of the averaged signal, while Tyler (1978) and Regan (cf. 1975a) among others prefer narrow bandpass filtering based on synchronous demodulation. Nelson *et al.* (1984) use phase-sensitive filtering via synchronous demodulation.

Since all these techniques are closely related and, under the right circumstances, give equivalent results, the ongoing discussion as to which method is "superior" to the other seems pointless. At the same time an imprecise use of signal processing terms has led to misleading or simply wrong assertions. In conclusion, I therefore want to point out the relationships and close with some remarks about the terminology.

The techniques can be categorized into phase-sensitive ("phase-locked") and phase-insensitive. For a specified bandwith, they give equivalent results within a group. In the *phase-insensitive* case, a narrow-band filter with center frequency f and bandwidth Δf, when fed with a stationary signal, will yield the same output amplitude and signal-to-noise ratio as given by the amplitude of the frequency component at f of a Fourier analysis with frequency resolution Δf. The FFT can be carried out over the raw EEG, or over averaged data.* The band-pass filter can be realized with conventional analog high- and low-pass filters or by synchronous demodulation, using, for example, a lock-in amplifier, together with a "quadrature" circuit calculating vector amplitude and phase. It can also be implemented as a digital program (excellent practical help for realizing digital filters is found in IEEE's "Programs for digital signal processing", 1979) or as firmware in a digital signal processing chip. As far as the *phase-sensitive* case is concerned, it is most interesting to note that phase-sensitive filtering corresponds to *projecting vectors of FFT results* onto some predefined main phase. Again, the phase-sensitive filter can be realized with analog multipliers, or as a digital program. You can also use a lock-in amplifier. One can turn phase-insensitive to phase-locked results by calculating the projections on some predefined phase angle, or go back by calculating the "quadrature" (i.e. r.m.s. or amplitude) function. Note that in the phase-sensitive case signals are both positive and negative, and noise is symmetric around zero (cf. Fig. 7), while in the phase-insensitive case the signal and noise are always positive (cf. Fig. 5).

The S/N ratio of a phase-sensitive method is better than for a comparable phase-insensitive method because more noise is rejected; to pass, noise must not only have the "right" frequency but also the "right" phase. The higher noise reduction is won by supplying additional knowledge about the signal, namely its phase. When the assumed phase is wrong, the method loses its effectiveness as a noise filter; it then also suppresses the signal.

The question remains what bandwidths and center frequencies are obtained in each case. The obtainable bandwidth is always inversely related to the meassurement time. For an analog filter this shows in its response lag,† for Fourier analysis in the necessary time interval over which the transform has to be calculated (cf. a previous paragraph). The proportionality constant of this relationship depends on the exact filter characteristic‡ but usually ranges between 0.5 and 2.

More filter characteristics can be realized with off-line processing than on-line. The reason lies in "filter-causality". During the measurement, a filter only has information about the signal's past, not about its future. Later, more information about the signal is available. The ideal rectangular bandpass is one of the filter functions which cannot be realized on-line.

Finally, some comments about the use of signal processing terminology seem appropriate. The distinction between Fourier analysis and filtering should not be blurred. A *filter* is a

---

*It thus makes little sense to say that Fourier analysis is 100 times faster than averaging (Regan, 1977a), or that averaging is inappropriate for analyzing steady state potentials (ib.). Fourier analysis and averaging can be sensibly combined, e.g. to reduce processing time (cf. previous paragraphs).

†Regan repeatedly states a bandwidth of his filter of "as low" as 0.001 Hz (1970, 1972, 1977a p. 111, 1977b p. 1476). Such a filter would have a response lag of 16 min, hardly what one would want for on-line VEP-tracking.

‡Let b denote bandwidth and t_a denote rise-time defined as

$$b = \frac{1}{2\pi}\int_0^\infty G(j\omega)^2\,d\omega$$

and

$$t_a = 1 \Big/ \int_0^\infty g^2(t)\,dt,$$

where $g(t)$ is the impulse and $G(j\omega)$ is the transfer function. Then

$$t_a = 1/(2b)$$

(Kaufmann, 1959).

dynamic system transforming a temporal signal into another temporal signal, with the transfer characteristic described in the frequency domain. A *Fourier transformation* translates a description in the time domain into a description in the frequency domain. Regan calls both his synchronous filter (defined e.g. in Regan, 1975a) and "a device based on a bank of narrow-band filters" a "Fourier analyser" (1977a, p. 114). The first use should be discouraged for the given reason. As to the second use, a filter-bank (together with its built-in integrators) should be less specifically called a "spectral analyser", which is also the term used by the manufacturers. The reason is that the center frequencies of the individual band-passes are hard-wired to certain values which is not the case for Fourier analysis.

Acknowledgements—I thank Ingo Rentschler, Martin Huebner, Stephen Pope, Lew Harvey, and Terry Caelli for their comments on the manuscript, and Hans Brettel for translation to French. Study supported by Fraunhofer-Gesellschaft, Grant InSan I-0784-V-6385 to I. Rentschler.

REFERENCES

Aunon J. I., McGillem C. D. and Childers D. (1981) Signal processing in evoked potentials research: Averaging and modelling. *Crit. Rev. Bioeng.* **5,** 323–367.

Batschelet E. (1965) *Statistical Methods for the Analysis of Problems in Animal Orientation and Certain Biological Rhythms.* Am. Inst. Biol. Sci.

Campbell F. W. and Maffei L. (1970) Electrophysiological evidence for the existence of orientation and size detectors in the human visual system. *J. Physiol., Lond.* **207,** 635–652.

Childers D. G. (1977) Evoked responses: Electrogenesis, models, methodology, and wavefront reconstruction and tracking analysis. *Proc. IEEE* **65,** 611–626.

Diamond A. L. (1977) Latency of the steady state visual evoked potential. *Electroenceph. Clin. Neurophysiol.* **42,** 125–127.

Fiorentini A., Pirchio M. and Spinelli D. (1983) Electrophysiological evidence for spatial frequency selective mechanisms in adults and infants. *Vision Res.* **23,** 119–127.

Hays W. L. (1963) *Statistics.* Holt, Rinehart & Winston, New York.

Keidel W. D. (1965a) Computed audio-encephalograms in man (a technique of "objective" audiometry). *Int. Audiol.* **4,** 56–60.

Keidel W. D. (1965b) Zur Frage der Korrelierbarkeit zwischen objektiver und subjektiver Sinnesphysiologie. In: *Informationsverarbeitung und Kybernetik. Studien und Berichte der Kath. Akademie in Bayern,* Vol. 32. Echter, Wuerzburg.

Levi D. M. and Harwerth R. S. (1978) A sensory mechanism for amblyopia: Electrophysiological studies. *Am. J. Optom. Physiol. Opt* **55,** 163–171.

Nelson J. I., Seiple W. H., Kupersmith M. J. and Carr R. E. (1984) Lock-in signal retrieval techniques for swept-parameter visual stimulation. *J. clin. Neurophysiol.* **1,** 409–436.

Petrig B. (1980) *Nachweis von Stereopsis bei Kindern mittels stochastischer Punktstereogramme und der dazugehoerigen evozierten Potentiale,* Thesis Diss. ETH Nr. 6685. Eidgenoessische Technische Hochschule Zuerich.

Regan D. (1975a) Colour coding of pattern responses in man investigated by evoked potential feedback and direct plot techniques. *Vision Res.* **15,** 175–183.

Regan D. (1975b) Recent advances in electrical recording from the brain. *Nature, Lond.* **253,** 401–407.

Regan D. (1977a) Fourier analysis of evoked potentials; some methods based on Fourier analysis. In: *Visual Evoked Potentials in Man: New Developments,* edited by Desmedt J. E., pp. 110–117. Clarendon Press, Oxford.

Regan D. (1977b) Rapid methods for refracting the eye and for assessing visual acuity in amblyopia, using steady-state visual evoked potentials. In: *Visual Evoked Potentials in Man: New Developments,* edited by Desmedt J. E., pp. 418–426. Clarendon Press, Oxford.

Regan D. (1977c) Steady state evoked potentials. *J. opt. Soc. Am.* **67,** 1475–1489.

Spekreijse H., Estevez O. and Reits D. (1977) Visual evoked potentials and the physiological analysis of visual processes in man. In *Visual Evoked Potentials in Man: New Developments,* edited by Desmedt J. E., pp. 16–89. Clarendon Press, Oxford.

Strasburger H. and Rentschler I. (1986) A digital fast sweep technique for studying steady state visual evoked potentials. *J. Electrophys. Tech.* **13,** 265–278.

Strasburger H., Scheidler W. and Rentschler I. (1986) Steady state visual evoked potentials and grating perception. To be published.

Tyler C. W., Apkarian P. and Nakayama K. (1978) Multiple spatial-frequency tuning of electrical responses from human visual cortex. *Expl Brain Res.* **33,** 535–550.

Tyler C. W., Apkarian P., Levi D. M. and Nakayama K. (1979) Rapid assessment of visual function: An electronic sweep technique for the pattern visual evoked potential. *Invest. Ophthal. Visual Sci.* **18,** 703–713.

Yin T. C. T., Kalil R. E. and Schechter P. B. (1983) Visual-evoked response from strabismic cats. *Invest. Ophthal. Visual Sci.* **24,** 1390–1399.

Zar J. H. (1974) *Biostatistical Analysis, Chap.* 22, *Circular Distributions.* Prentice Hall, Englewood Cliffs, N.J.